

# Spontaneous Formation of Giant Bioactive Protein-Block Copolymer Vesicles in Water

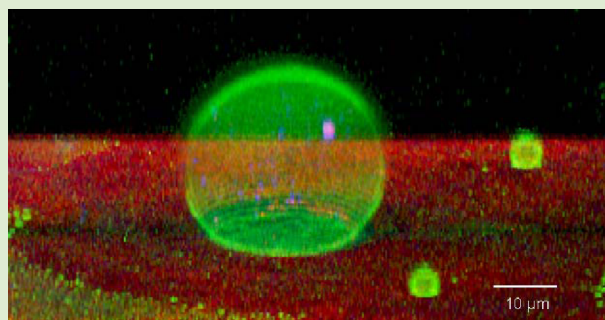
Elkin Amado,<sup>†</sup> Regina Schöps,<sup>†</sup> Wolfgang Brandt,<sup>‡</sup> and Jörg Kressler<sup>\*,†</sup>

<sup>†</sup>Institute of Chemistry, Martin Luther University Halle-Wittenberg, Von-Danckelmann-Platz 4, D-06120 Halle (Saale), Germany

<sup>‡</sup>Department of Bioorganic Chemistry, Leibniz Institute of Plant Biochemistry, Weinberg 3, D-06120 Halle (Saale), Germany

## S Supporting Information

**ABSTRACT:** A novel strategy for the formation, without the need for organic solvents, of stable giant proteopolymersomes from the highly water-soluble triblock copolymer poly(2,3-dihydroxypropyl methacrylate)-*b*-poly(propylene oxide)-*b*-poly(2,3-dihydroxypropyl methacrylate) and the protein assembly streptavidin (SAv)-biotin-bovine serum albumin is presented. The method yields bioactive polymersomes with sizes in the tens of micrometers range having an SAv-functionalized membrane, thus, offering binding sites for a broad range of biotin conjugates. The vesiculation mechanism and the distribution of polymer and proteins in the proteopolymersomes membrane are investigated by confocal laser scanning microscopy and supported by molecular dynamic simulations.



Preparing a synthetic mimic of a living cell is a persistent challenge to science to which many efforts have been dedicated. A first step was the production of liposomes, vesicles formed from phospholipid bilayers, thus, resembling the basic constitutional element of natural cell membranes. A great improvement of the stability and lifetime, two of the main drawbacks of liposomes, was achieved with the discovery that some amphiphilic synthetic polymers are also able to form unilamellar vesicles, so-called polymersomes.<sup>1</sup> They have sizes in the hundreds of nanometers to tens of micrometers range and membrane thickness in the order of 10–20 nm, that compared with a 4–5 nm thickness of a lipid membrane explains their higher mechanical stability and reduced permeability compared to liposomes.<sup>2</sup> Polymersomes are currently being evaluated as drug and gene delivery systems<sup>3</sup> and as nanoreactors.<sup>4</sup> A further step toward mimicking a living cell was the incorporation of membrane proteins with the aim of furnishing polymersomes with functionalities proper of cells, leading to biohybrid proteopolymersomes.<sup>5–7</sup>

Despite their advantages compared to conventional liposomes and increasing research efforts, the number of polymersomes available for the production of polymersomes is still limited and only some polymer families are known to be suitable, such as polystyrene-*b*-poly(acrylic acid),<sup>1</sup> poly(ethylene oxide)-*b*-polystyrene (PEO-*b*-PS),<sup>8</sup> poly(2-ethyl-2-oxazoline)-*b*-poly(dimethylsiloxane)-*b*-poly(2-ethyl-2-oxazoline),<sup>5</sup> poly(2-methyloxazoline)-*b*-poly(dimethylsiloxane)-*b*-poly(2-methyloxazoline),<sup>6</sup> and poly(ethylene oxide)-*b*-poly(butadiene) (PEO-*b*-PBD),<sup>9</sup> among others. Besides, not all copolymers within one of these families fulfill the requirements for vesicle formation. In particular, the balance between hydrophilic and lipophilic

blocks must be such that the formation of lamellar phases is promoted over micellization. Typically, a ratio ( $f$ ) of the mass of hydrophilic moieties to total mass within the range of 25–45% is required.<sup>10</sup>

Additional obstacles for the widespread use of polymersomes arise from the preparation methods available. Conventionally, methods originally developed for the production of liposomes, such as hydration of thin films, extrusion of multilamellar vesicles dispersions, inverted emulsion, and electroformation, have been adopted.<sup>11</sup> Unfortunately, some of them impose the use of organic solvents whose residues might pose a serious drawback for biomedical applications. Furthermore, the size of the obtained polymersomes depends strongly on the preparation method. It ranges from some hundred nanometers for small rehydrated or extruded vesicles to tens of micrometers for giant electroformed vesicles. The smaller vesicle sizes preclude the use of optical microscopy techniques and impose the more demanding electron microscopy for investigations. Also, information regarding mechanical properties or detailed morphology of the vesicle membrane (as obtained through micropipet techniques<sup>12</sup> and fluorescence microscopy,<sup>13</sup> respectively) is better accessible with micrometer-size vesicles. Therefore, it is highly desirable that giant vesicles be readily available for biomedical research.

In this study, we present a novel water-based (organic solvent-free) straightforward method for the formation of giant unilamellar proteopolymersomes from a highly water-soluble

Received: June 13, 2012

Accepted: July 19, 2012

Published: July 20, 2012

nonionic amphiphilic copolymer and a protein layer. Specifically, vesicles of the triblock copolymer PGM-PPO (see chemical structure in Figure 1a) having a hydrophobic

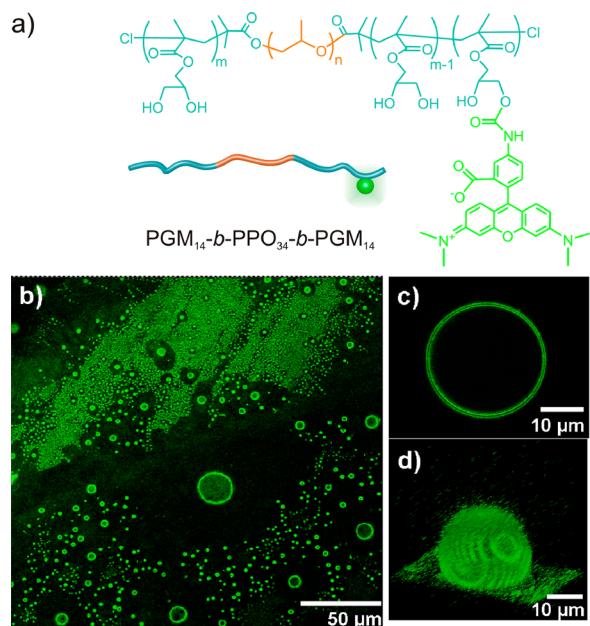


**Figure 1.** (a) Molecular structure of fluorescent-labeled PGM-PPO block copolymer. (b–d) CLSM images showing typical distribution and sizes of giant proteopolymersomes three days after PGM-PPO (33  $\mu\text{M}$ ) addition on top of protein-coated glass supports: (b) surface overview, (c) equatorial cross-section of a vesicle, and (d) corresponding 3D reconstruction from single vertical stacks.

PPO middle block and two hydrophilic poly(glycerol monomethacrylate), PGM also known as poly(2,3-dihydroxypropyl methacrylate), outer blocks, and the protein assembly streptavidin–biotin–bovine serum albumin (SAv–biotin–BSA) are formed spontaneously in water after adsorption of the polymer onto surfaces coated by a film of the proteins. The method yields bioactive proteopolymersomes having an SAv-functionalized membrane, thus, offering binding sites for biotin. Such ligand–receptor pair SAv–biotin exhibits a high affinity, being one of the strongest noncovalent bonds known in nature, and finds widespread use in biomedicine. The obtained proteopolymersomes have sizes in the tens of micrometers range, which enabled us to investigate the vesiculation mechanism and the distribution of polymer and proteins in the membrane by direct observation through confocal laser scanning microscopy (CLSM).

PGM-PPO was synthesized by atom transfer radical polymerization (ATRP), as described previously.<sup>14</sup> A fluorescent tetramethylrhodamine (TMR) label was attached by reacting on average one primary hydroxyl group in the PGM blocks per polymer chain with TMR-5-carbonyl azide. Experimental details are given in the Supporting Information. PGM is biocompatible<sup>15</sup> and possesses high water affinity. On the other hand, PPO exhibits lower critical solution temperature (LCST) phase behavior and the cloud point of PPO<sub>34</sub> is around 10 °C. This makes PGM-PPO, as a whole, thermoresponsive. With increasing temperature, the middle block becomes insoluble in water, triggering a self-assembly process. However, due to its very high hydrophilic ratio ( $f \sim 70\%$ ) and the weak hydrophobicity of PPO,<sup>10</sup> PGM-PPO forms

micelles rather than vesicles in water. Such micelles with a mean diameter of 20 nm have a PPO core surrounded by a PGM corona.<sup>14</sup> The corresponding critical micelle concentration (cmc) at 25 °C is  $1.35 \times 10^{-4}$  M (135  $\mu\text{M}$ ), as determined by isothermal titration calorimetry (ITC, Figure S1, Supporting Information).

In a first series of experiments, giant polymersomes were formed onto glass supports previously passivated with BSA/biotinylated BSA (10:1 molar ratio) and subsequently coated by incubation with SAv (see details in the Supporting Information). After rinsing to remove nonattached proteins from the support, an aqueous solution of PGM-PPO (33–330  $\mu\text{M}$  final concentration) was added. Typically, spherical vesicles with diameters up to 25  $\mu\text{m}$  (Figure 1b) were spontaneously formed without any mechanical or thermal stimulus within 5 min to 2 h of incubation depending on PGM-PPO concentration. They were stable for weeks when stored between 4 °C and room temperature. Control experiments on glass supports without passivation or coating did not exhibit vesicle formation indicating that vesiculation is induced by the presence of the protein layer. Besides, experiments with unlabeled PGM-PPO and a fluorescent labeled SAv (Figure S2, Supporting Information) confirmed that the formation of vesicles was not due to the TMR label. The broad size distribution of the vesicles and their particular arrangement (Figure 1b), with large vesicles surrounded by areas depleted from smaller ones, suggests that vesicles grew by a coalescence mechanism. However, since no vesicle fusion event was directly observed, Ostwald-ripening<sup>16</sup> cannot be discarded. An equatorial cross-section of a vesicle (Figure 1c) evidences the unilamellarity of its membrane.

To investigate the spatial distribution of polymer and proteins in the membrane, experiments with cyanine (Cy5) fluorescent-labeled SAv were carried out. As shown in Figure 2a,b, both PGM-PPO and SAv were present throughout the vesicle, although their distribution was not homogeneous. SAv

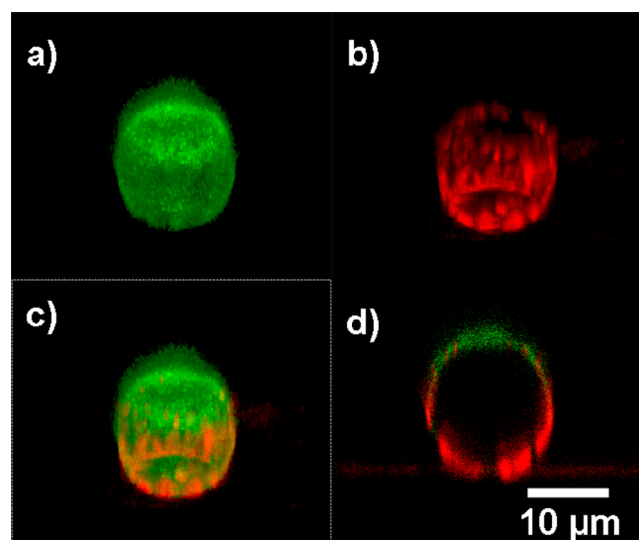


**Figure 2.** Spatial distribution of PGM-PPO (green) and SAv (red) in the proteopolymersomes. 3D reconstructions from separated fluorescence channels: (a) PGM-PPO, (b) Cy5-SAv, (c) overlay. (d) Vertical cross-section of the same vesicle (from a single vertical scan previous to the z-stack capture), exhibiting a surface density gradient of SAv from bottom to top. Vesicle imaged 15 min after PGM-PPO (33  $\mu\text{M}$ ) addition.

localized preferentially in the bottom half, while the top half was richer in PGM-PPO. A vertical cross-section (Figure 2d) appeared to suggest a morphology similar to a Janus vesicle,<sup>17</sup> that is, having a sharp border between the two zones. However, this first impression was refuted by a 3D reconstructed overlay image from a z-stack capture (Figure 2c), which presents a rather gradual transition from an SAV-rich region to a PGM-PPO one, clearly evidencing a surface gradient of SAV from bottom to top.

The ability of the SAV functionalized proteopolymersomes to further bind biotinylated probes was examined in experiments with addition of fluorescent labeled (Alexa Fluor 594) biotin to previously formed vesicles (Figure S3, Supporting Information). It was verified that SAV retained its functionality after vesiculation and that fluorescent biotin remains bound even after exchanging the external solution by pure water (Figure S4, Supporting Information). Additionally, ITC experiments on the binding of biotin to SAV, alone or in the presence of very high concentrations (344  $\mu\text{M}$ ) of PGM-PPO, evidenced only a limited influence of PGM-PPO on the binding process (Figure S5, Supporting Information).

Due to the high affinity of the SAV-biotin pair, it is not expected that the adsorption of PGM-PPO onto the SAV-biotin-BSA layer could break this complex. To verify this assumption passivation was also carried out with fluorescein-labeled BSA (FITC-BSA), which allowed us to investigate the distribution of each protein separately. An overview of the support surface during vesiculation (Figure 3a) reveals that the

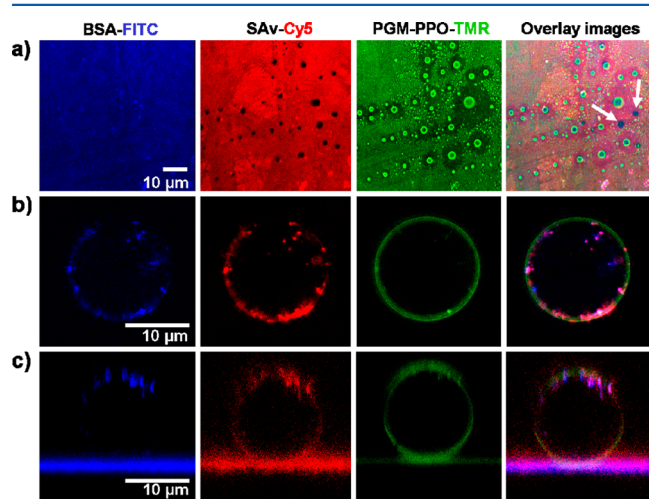


**Figure 3.** Distribution of BSA (blue), SAV (red), and PGM-PPO (green) in the membrane. From top to bottom: (a) surface overview, (b) equatorial cross-section, and (c) vertical cross-section. Arrows in the surface overlay image indicate the original position of vesicles subsequently detached from the surface. Vesicles imaged 1 h after PGM-PPO (100  $\mu\text{M}$ ) addition.

BSA layer remains almost intact, while areas depleted of SAV are found at places where vesicles were formed. Footprints left behind by vesicles detached from the surface can be identified in the overlay image (see arrows in Figure 3a). Equatorial (Figure 3b) and vertical cross sections (Figure 3c) of a vesicle exhibit a magenta color in the overlay images that confirms a spatial overlap (colocalization) of BSA and SAV.

To elucidate the molecular interaction between PGM-PPO and the SAV upmost layer during the initial adsorption step molecular modeling studies were carried out. Since the protein

surface possesses both hydrophobic and hydrophilic regions (Figure 4b) interactions with the hydrophobic PPO block as

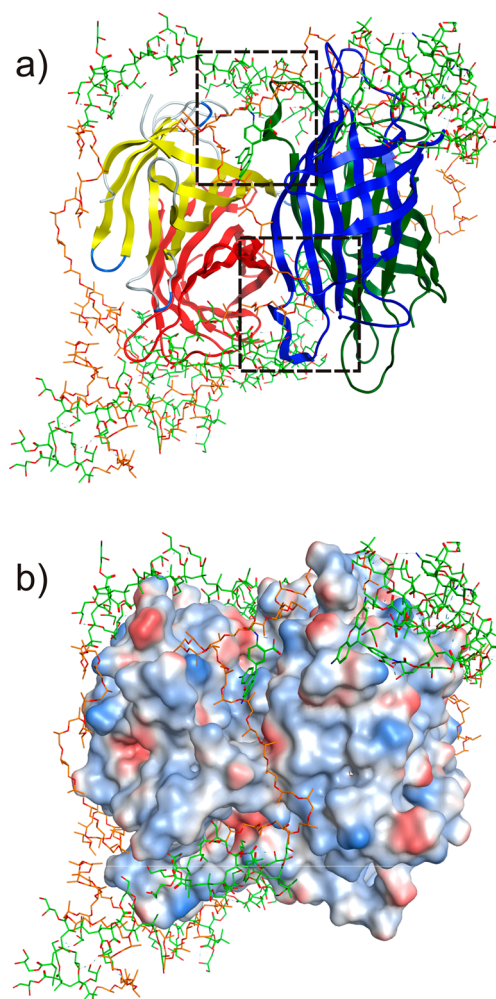


**Figure 4.** Final structure after 5 ns MD simulation of four PGM-PPO chains bound to tetrameric SAV in a periodic boundary water box. (a) Crystallographic 3D structure of the SAV tetramer. The PGM blocks (green) bind deeply around the biotin binding gorges of SAV (dashed boxes) while the hydrophobic PPO blocks (orange) are extended across the SAV surface. (b) Corresponding SAV surface potentials. Hydrophilic regions are colored blue, hydrophobic red. Water molecules were omitted for clarity.

well as through the hydrophilic PGM blocks could be expected. Docking analyses allowed identifying the most probable interaction sites. It is concluded that PGM blocks are favored for interaction with the protein, particularly through hydrogen bonding around the biotin binding gorge of SAV (see dashed boxes in Figure 4a). Interestingly, some PGM interaction areas closely match the binding sites preferred by glycerol when cocrystallized with SAV (Figures S6,7, Supporting Information). Molecular dynamic (MD) simulations performed to evaluate the stability of SAV-PGM-PPO assemblies reveal that PGM blocks remain deeply bound to the protein, while PPO blocks are spanned between the PGM interaction sites. Thus, an upper PGM-PPO layer is formed and bound to the SAV layer underneath through the PGM blocks. The high water affinity of PGM creates an osmotic pressure inside the protein layer providing a driving force for vesiculation, as discussed below.

A model of the vesiculation mechanism based on the results obtained in this study is illustrated in Figure 5. After adsorption

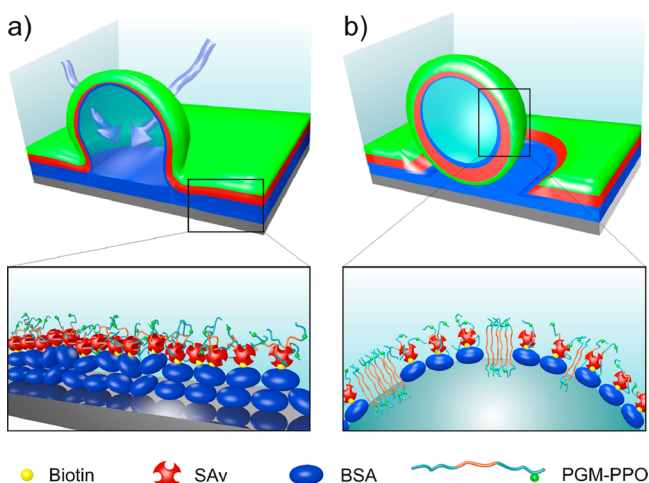


**Figure 5.** Illustration of the proposed vesiculation mechanism. (a) Hydration and swelling of the protein film with adsorbed PGM-PPO. Water diffusion is represented by arrows. The inset illustrates the initial layered arrangement obtained after polymer adsorption (PGM-PPO layer is colored green, SAv layer red, BSA layer blue). (b) Fully developed vesicle. The inset shows the final structure of the vesicles' membrane.

of PGM-PPO onto the protein-coated glass support, a layered structure is obtained with the polymer on top (inset in Figure 5a). This initial step is followed by the diffusion of water into the film (arrows in Figure 5a) and its concomitant swelling as a consequence of the osmotic pressure inside the layered structure. Such process resembles the rehydration of dry lipid films during liposome formation.<sup>18</sup> An additional factor contributing to vesicle formation is the tendency of deposited BSA to stack in multilayers,<sup>19</sup> which also explains why only a superficial layer of proteins (Figure 5b) is incorporated in the vesicles' membrane.

In summary, a novel strategy for the formation of stable giant proteopolymersomes from highly water-soluble nonionic amphiphilic copolymers and a protein layer without the need for organic solvents was developed. The method could be extended to other families of amphiphilic polymers which are currently unsuitable for the preparation of polymersomes as a consequence of a too large hydrophilic ratio. For example, most of the water-soluble members of the Pluronic class of block copolymers (PEO-*b*-PPO-*b*-PEO) are unable to form vesicles, but only micelles and solely the most hydrophobic Pluronic can be used to produce polymersomes.<sup>9</sup> Our strategy yields proteopolymersomes functionalized with SAv that might be further complexed with some of the many commercially available biotin-conjugates, such as biotinylated antibodies, enzymes, nucleotides, phospholipids, dextrans, fluorophores, quantum dots, or PEO-biotin, or be attached to a biotinylated surface. Besides, the meridional composition gradient exhibited by the vesicles might open a route to study effects arising from changes of the protein surface density on the conjugation of biotinylated probes. These facts together foresee multiple possibilities for the application of the obtained SAv-functionalized giant polymersomes in biomedical research and represent an important step toward the creation of synthetic mimics of living cells.

## ■ ASSOCIATED CONTENT

### 📄 Supporting Information

Materials, instrumentation, methods, and ITC results. This material is available free of charge via the Internet at <http://pubs.acs.org>.

## ■ AUTHOR INFORMATION

### Corresponding Author

\*E-mail: [joerg.kressler@chemie.uni-halle.de](mailto:joerg.kressler@chemie.uni-halle.de)

### Notes

The authors declare no competing financial interest.

## ■ ACKNOWLEDGMENTS

This work was supported by DFG (FOR 1145). We thank T. Wiczorek for some of the graphic art work.

## ■ REFERENCES

- (1) Zhang, L.; Eisenberg, A. *Science* **1995**, *268*, 1728–1731.
- (2) Le Meins, J. -F.; Sandre, O.; Lecommandoux, S. *Eur. Phys. J. E* **2011**, *34*, 14.
- (3) Christian, D. A.; Cai, S.; Bowen, D. M.; Kim, Y.; Pajeroski, J. D.; Discher, D. E. *Eur. J. Pharm. Biopharm.* **2009**, *71*, 463.
- (4) Tanner, P.; Baumman, P.; Enea, R.; Onaca, O.; Palivan, C.; Mier, W. *Acc. Chem. Res.* **2011**, *44*, 1039–1049.
- (5) Choi, H.-J.; Montemagno, C. D. *Nano Lett.* **2005**, *5*, 2538–2542.
- (6) Kumar, M.; Grzelakowski, M.; Zilles, J.; Clark, M.; Meier, W. *Proc. Natl. Acad. Sci. U.S.A.* **2007**, *104*, 20719–20724.
- (7) Nallani, M.; Andreasson-Ochsner, M.; Tan, C. D.; Sinner, E.-K.; Wisantoso, Y.; Geifman-Schochat, S.; Hunziker, W. *Biointerphases* **2011**, *6*, 153–157.
- (8) Kim, K. T.; Zhu, J.; Meeuwissen, S. A.; Cornelissen, J.; Pochan, D. J.; Nolte, R.; van Hest, J. *J. Am. Chem. Soc.* **2010**, *132*, 12522–12524.
- (9) Rodríguez-García, R.; Mell, M.; López-Montero, I.; Netzel, J.; Hellweg, T.; Monroy, F. *Soft Matter* **2011**, *7*, 1532–1542.
- (10) Discher, D. E.; Eisenberg, A. *Science* **2002**, *297*, 967–973.
- (11) Walde, P.; Consentino, K.; Engel, H.; Stano, P. *ChemBioChem* **2010**, *11*, 848–865.
- (12) Mabrouk, E.; Cuvelier, D.; Pontani, L.-L.; Xu, B.; Levy, D.; Keller, P.; Brochard-Wyart, F.; Nassoy, P.; Li, M.-H. *Soft Matter* **2009**, *5*, 1870–1878.
- (13) LoPresti, C.; Massignani, M.; Fernyhough, C.; Blanz, A.; Ryan, A. J.; Madsen, J.; Warren, N. J.; Armes, S. P.; Lewis, A. L.; Chirasatsin, S.; Engler, A. J.; Battaglia, G. *ACS Nano* **2011**, *5*, 1775–1784.
- (14) Amado, E.; Augsten, C.; Maeder, K.; Blume, A.; Kressler, J. *Macromolecules* **2006**, *39*, 9486–9496.
- (15) Wang, C.; Yu, B.; Knudsen, B.; Harmon, J.; Moussy, F.; Moussy, Y. *Biomacromolecules* **2008**, *9*, 561–567.
- (16) Taylor, P. *Adv. Colloid Interface Sci.* **1998**, *75*, 107–163.
- (17) Beales, P. A.; Nam, J.; Vanderlick, T. K. *Soft Matter* **2011**, *7*, 1747–1755.
- (18) Battaglia, G.; Ryan, A. J. *Nat. Mater.* **2005**, *4*, 869–876.
- (19) Terashima, H.; Tsuji, T. *Colloids Surf., B* **2002**, *27*, 115–122.